ELSEVIER

Journal of Structural Geology 28 (2006) 376–391

JOURNAL OF STRUCTURAL GEOLOGY

www.elsevier.com/locate/jsg

The role of deformation bands, stylolites and sheared stylolites in fault development in carbonate grainstones of Majella Mountain, Italy

Emanuele Tondi [a,*], Marco Antonellini [b], Atilla Aydin [b], Leonardo Marchegiani [a], Giuseppe Cello [a]

[a] *Department of Earth Sciences, University of Camerino, Via Gentile III da Varano, 62032 Camerino MC, Italy*
[b] *Department of Geological and Environmental Sciences, Stanford University, Stanford, CA 94305, USA*

Received 19 July 2005; received in revised form 14 November 2005; accepted 2 December 2005
Available online 2 February 2006

Abstract

In this paper we document deformation processes in porous carbonate grainstones of Cretaceous age in Majella Mountain in the central Apennines of Italy by detailed mapping of meso- and microstructural features as well as thin section observations and image analyses. We distinguished three main deformation mechanisms: (i) deformation bands developed by compaction and shear strain localization, (ii) stylolites formed by pressure solution, and (iii) subsequent shearing of stylolites. The deformation bands occur in six sets: five sets are compactive shear bands at high angles to bedding and one, which is the oldest, occurs parallel to bedding and is interpreted to be a compaction band. Stylolites localize along and within all six sets of deformation bands and are commonly sheared, as evidenced by striated surfaces and detectable offsets. These sheared stylolites are in many cases associated with one or two sets of subsidiary stylolites, oblique to the major set. The band-parallel sheared stylolites, together with the associated oblique sets of stylolites, form a tabular zone of fine grained cataclastic material within the compactive shear bands and accommodate slip in the range of 5–75 cm.

The bed-parallel compaction bands and bed-parallel stylolites, which are kinematically compatible, are interpreted to be pre-tilting structures developed in response to the overburden, whereas the five sets of compactive shear bands and the associated stylolites and sheared stylolites likely occurred during the syn- and post-tilting deformation phases recorded in the Majella anticline.

Keywords: Failure modes; Compaction bands; Compactive shear bands; Stylolites; Slip surfaces; Apennines

1. Introduction

Previous studies have pointed out the significant role played by pressure solution in deformation of carbonate rocks (for reviews see Rutter (1983) and Groshong (1988)). How pressure solution and the subsequent shearing of solution surfaces (referred to as stylolites in this paper) are responsible for fault development in carbonate rocks has also been discussed by several workers, including Alvarez et al. (1978), Engelder and Marshak (1985), Peacock and Sanderson (1995), Willemse et al. (1997), Salvini et al. (1999) and Billi et al. (2003). Graham et al. (2003) have recently documented a new faulting mechanism in platform carbonates of Majella Mountain, in which multiple sets of stylolites and their subsequent shearing result in progressively evolving normal faulting. This mechanism produces zones of fragmentation, breccia and fault rock (gouge) leading to through-going mature normal fault structures.

In clastic rocks, deformation bands are common structures where localized strains accumulate within narrow bands (Engelder, 1974; Aydin, 1978; Aydin and Johnson, 1978; Jamison and Stearns, 1982; Antonellini et al., 1994). The micromechanics of this type of strain localization includes pore collapse, grains fracturing and dissolution at grain to grain contacts (Aydin et al., in press). All these micromechanical processes give rise to small but detectable displacement discontinuities, typically from a few millimetres to a few centimetres across individual bands, whereas larger displacement discontinuities are accommodated by wide zones of multiple, composite deformation bands and slip surfaces (Aydin and Johnson, 1978; Antonellini et al., 1994; Mair et al., 2000; Shipton and Cowie, 2001).

In this paper, we report the occurrence of several sets of deformation bands in carbonate rocks of Majella Mountain and discuss their significance (see also Van Dijk et al., 2002, submitted for publication; Marchegiani et al., in press). In addition, we recognized stylolites formed by pressure solution

* Corresponding author. Tel.: +39 3204381432; fax: +39 0737402644.
E-mail address: emanuele.tondi@unicam.it (E. Tondi).

0191-8141/$ - see front matter © 2006 Elsevier Ltd. All rights reserved.
doi:10.1016/j.jsg.2005.12.001

within the previously formed deformation bands. Through detailed mapping at various scales and laboratory analyses of representative fault rock samples, we document how shearing of these stylolites within the bands produce zones of intense deformation, leading to the development of cataclastic fault rock. We also attempt to relate the observed change of the deformation processes from deformation banding to pressure solution to evolving mechanical behaviour of the deformed rock and the syn- and post-tilting deformation phases of Majella Mountain.

2. Geological setting

Majella Mountain is a thrust-related, asymmetric, box-shaped anticline (Fig. 1a and b) composed of carbonates of Lower Cretaceous–Miocene age, covered by a silicoclastic sequence of Upper Miocene–Middle Pliocene age (Fig. 1c). In map view, the anticline shows an arcuate shape oriented along an axis curving from the NW in the northern part and to NE in the southern part. The fold is periclinal in form and plunges gently to the northwest.

The Cretaceous sequence is composed of lagoonal platform limestones in the south, basinal carbonates in the north, with platform margin sediments across the centre of the anticline (Fig. 1c) (Eberli et al., 1993; Lampert et al., 1997). In post-Cretaceous times, the platform margin ceased to be active and a carbonate ramp sequence developed.

The internal deformation of the Majella anticline consists predominantly of normal faulting with some minor strike-slip faulting (Marchegiani et al., in press). Evidence of small scale compressional features, such as small folds and thrusts, is rare. The timing of the faulting, in relation to development of the

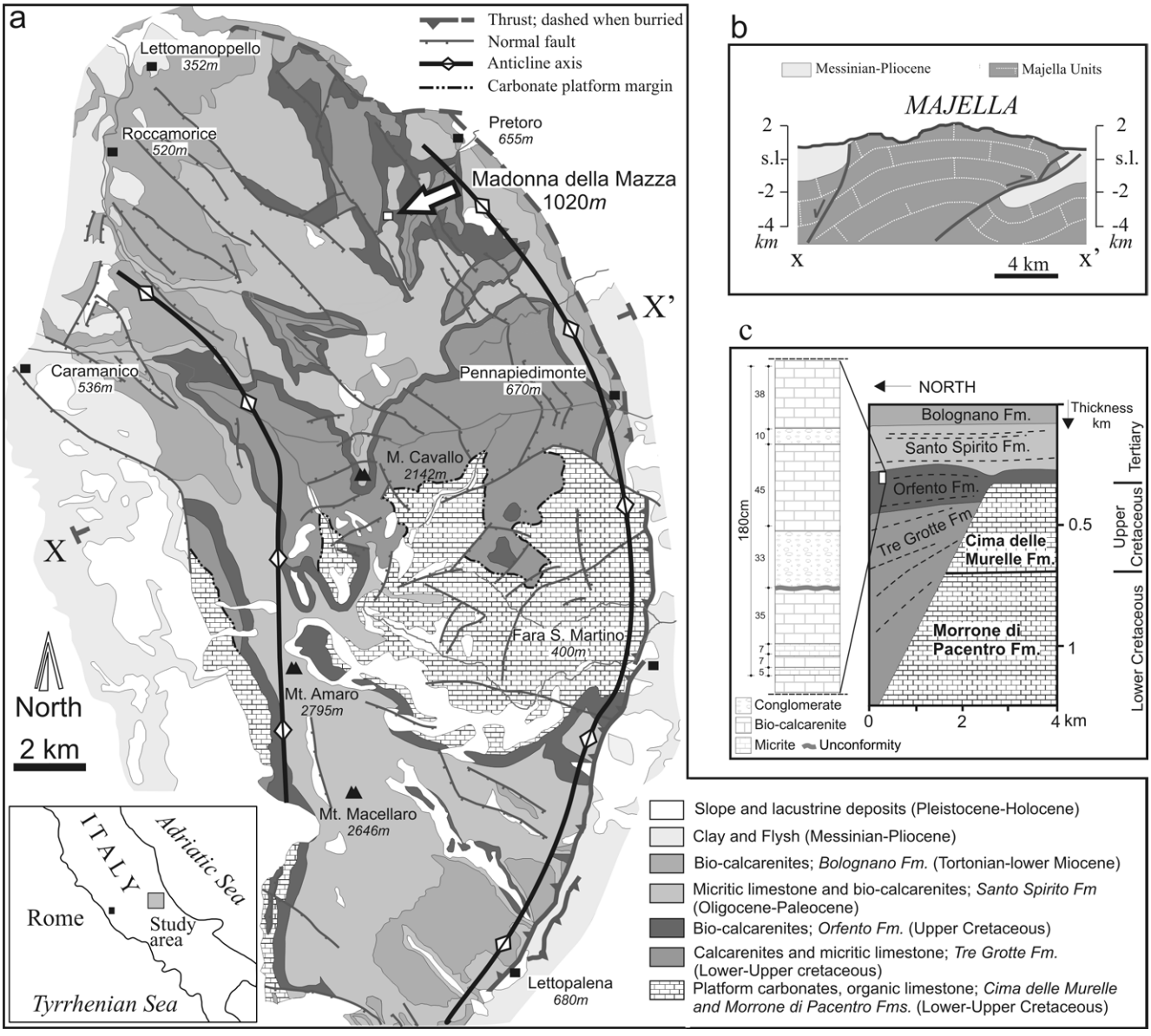

Fig. 1. (a) Geological map of Majella Mountain showing location of the study (white arrow). (b) Schematic cross-section across the Majella box-shaped anticline. (c) Stratigraphic section through the Majella platform margin and exposed stratigraphic section in the Madonna della Mazza quarry.

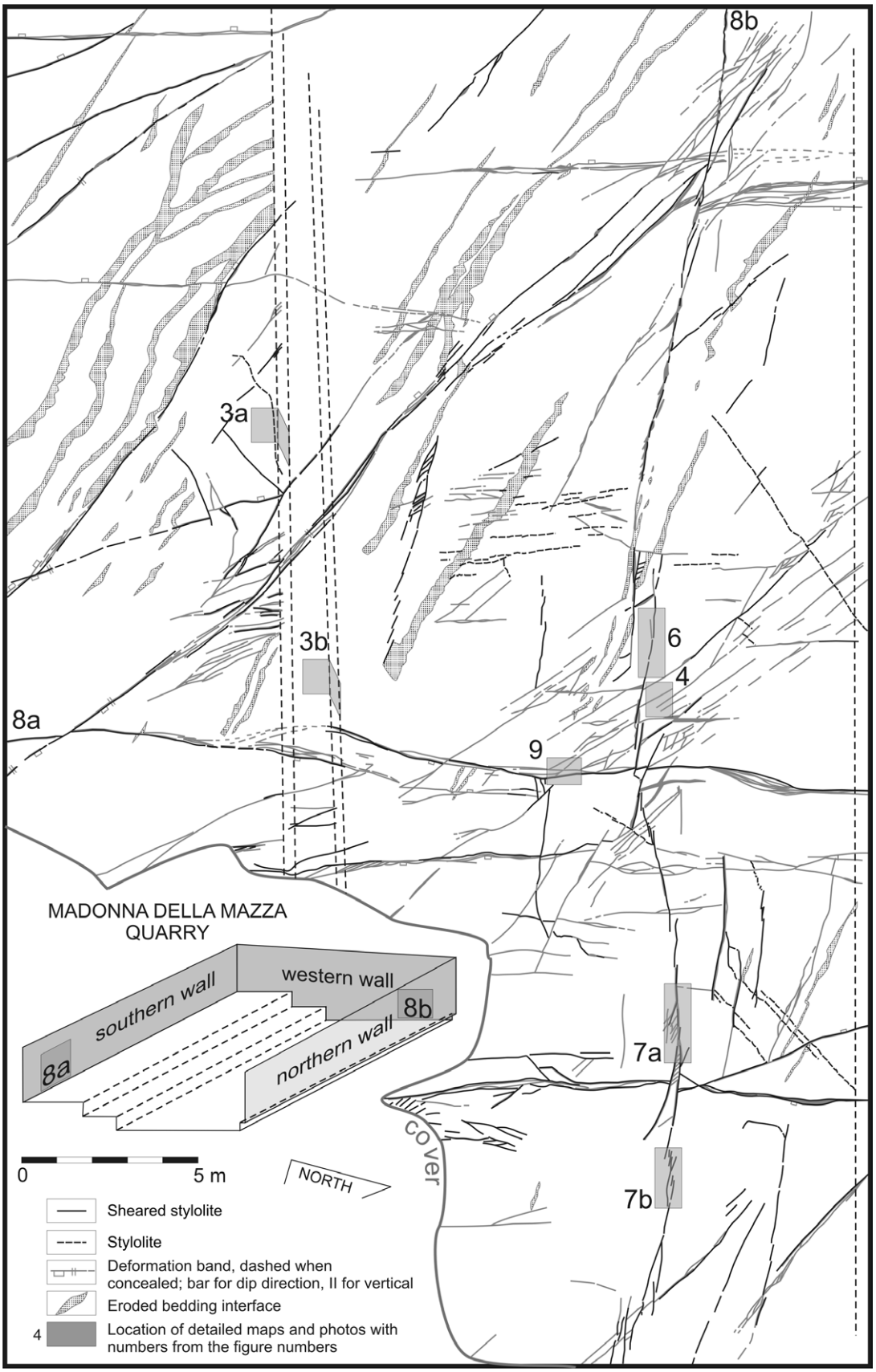

Fig. 2. Structure map of the pavement of the Madonna della Mazza quarry. The inset shows 3D quarry setting. Gray-shaded rectangles and the adjacent numbers show the locations and numbers of the figures of detailed maps and photographs.

Majella box-shaped anticline, has been placed in the Middle–Upper Pliocene (Ghisetti and Vezzani, 2002; Scisciani et al., 2002).

The location for the present study is a small quarry named Madonna della Mazza, which is situated on the inner part of the forelimb of the Majella anticline (Fig. 1a). There, the basinal sediments are represented by calcareous turbidites of the Orfento Formation (Fig. 1c). The Orfento Formation is Campanian to Maastrichtian in age, is composed of eroded subangular rudist fragments ranging in size from silt to rudite and includes some intercalated megabreccias (Mutti, 1995). The Formation covers the underlying platform margin and is a ramp succession, thickening to the north.

Bedding surfaces are represented by unconformities between grainstone beds and lenticular carbonate conglomerate levels (detailed column in Fig. 1c). These surfaces, which are in many cases striated, define tabular portions of rocks that typically range between 5 and 50 cm in thickness. They gently dip towards the NE with a mean orientation of 020°/10°. The high porosity of the grainstones, ranging between 15 and 30%, is attributed to a lack of cement during and after their deposition in a high energy marine environment (Mutti, 1995).

3. Field observations

The Madonna della Mazza quarry exposes a pavement floor and three subvertical walls, oriented north, south and west (Fig. 2, inset). The eastern side of the quarry is open. The quarry is 80 m long (east–west), and 50 m wide (north–south) with walls rising to a maximum height of about 12 m. Two pavement levels are exposed at the basement of the quarry; a larger, lower one in the northern part, and a smaller, somewhat higher one along the southern side. The two pavements are connected by two short, vertical walls with a narrow step in between. A map of the two pavements (Fig. 2) was constructed at 1:25 scale, using string line and detailed rectangular grid methods. In addition, detailed maps at 1:1 scale were constructed by utilizing acetate sheets taped directly onto the outcrops. The locations of these detailed maps are marked on

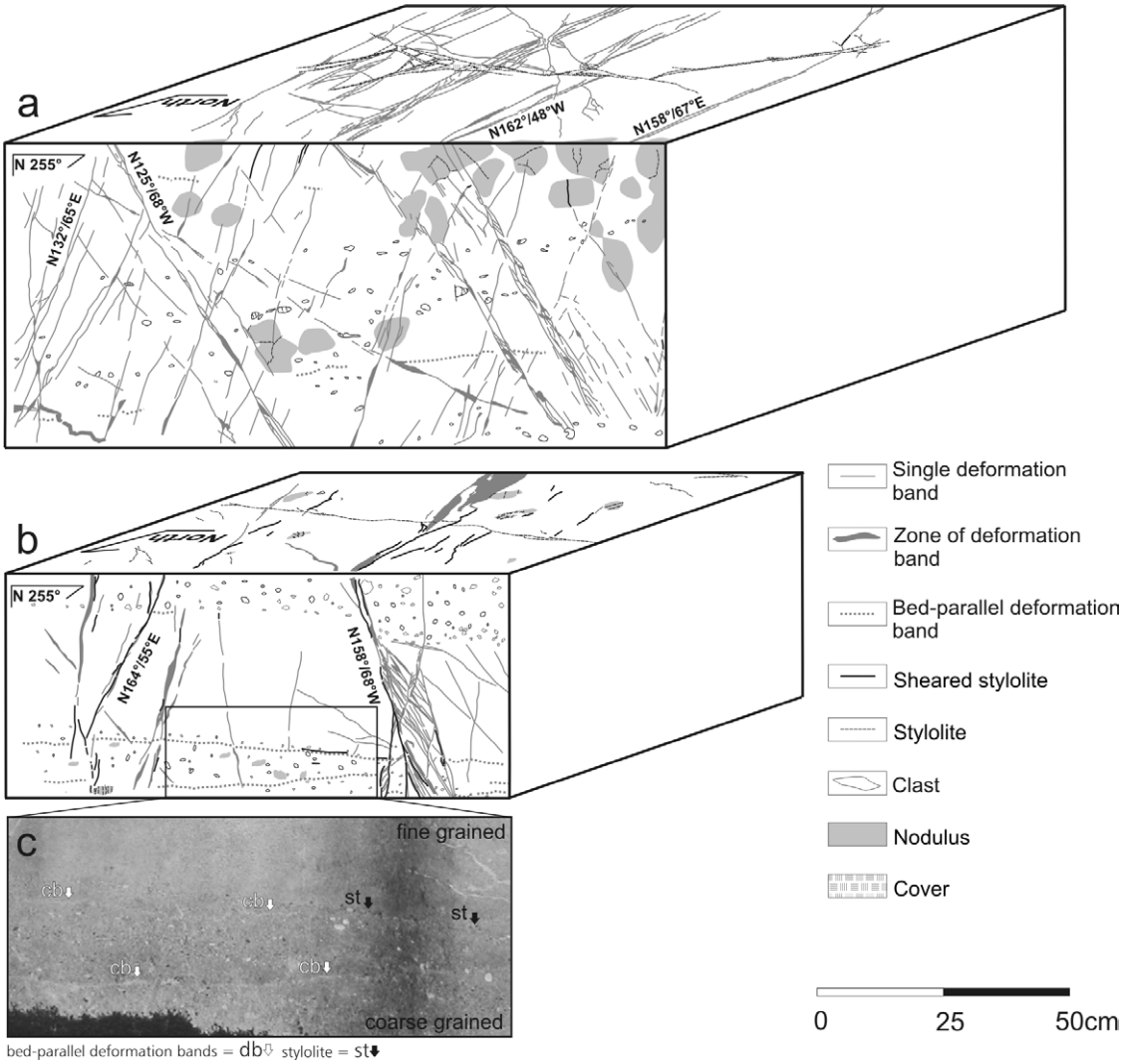

Fig. 3. (a) and (b) Block diagrams showing the six sets of deformation bands. (c) A photograph of lower part of (b) (see rectangle in (b) for location), showing bed-parallel deformation bands and stylolites. White and black arrows mark bed-parallel bands and stylolites, respectively.

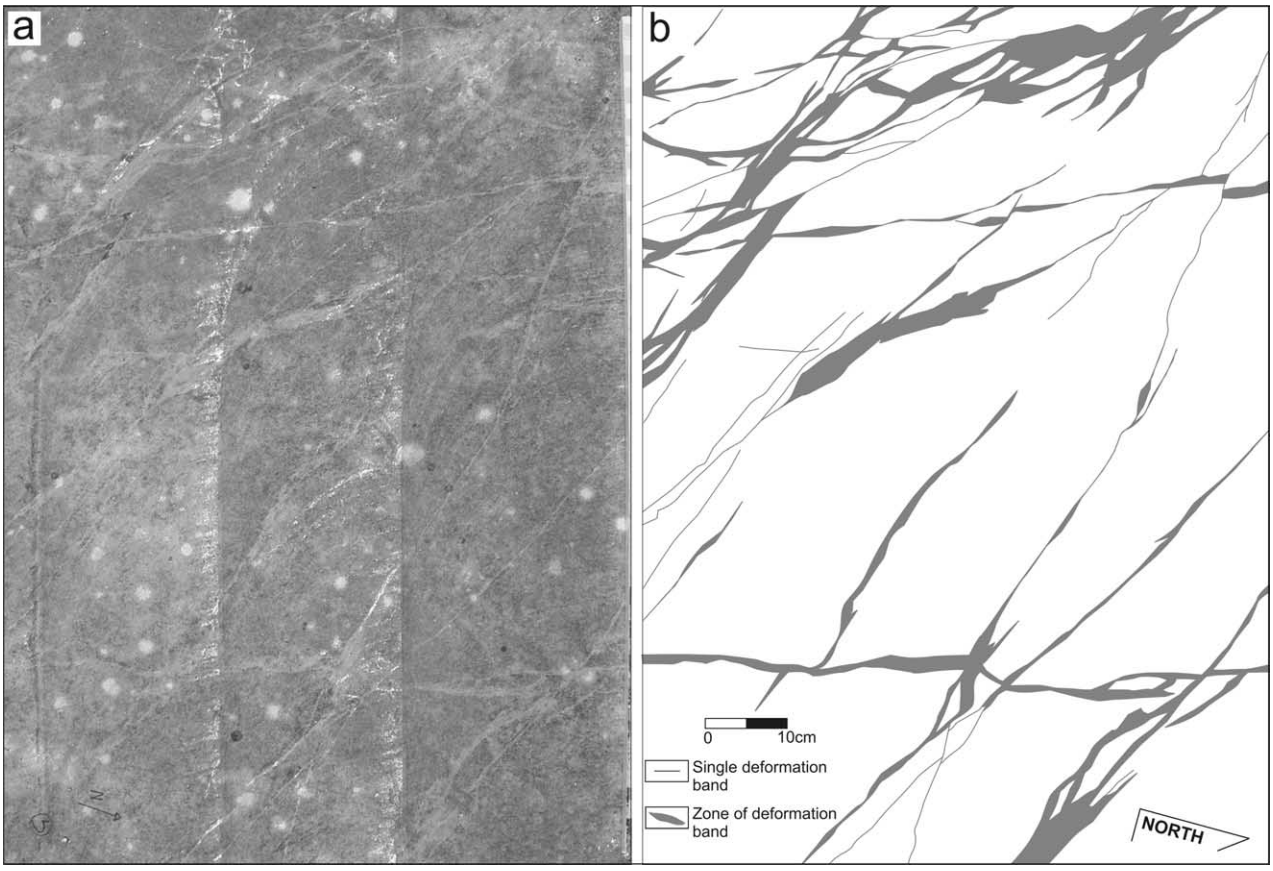

Fig. 4. N–NW and W–NW striking deformation bands; (a) photograph and (b) map. The mutually cross-cutting relationships show that they formed contemporaneously.

Fig. 2, but the actual maps and photographs are presented in separate figures as they are introduced.

In the Madonna della Mazza quarry we have identified six sets of deformation bands. The oldest set of these occurs parallel to the bedding and is consistently offset by other deformation bands. The bed-parallel deformation bands generally form within the coarse-grained beds, which are characterized by conglomerates with clasts ranging in size from 3 to 10 mm (Fig. 3). These bands have the same appearance as the other deformation bands, except that they show no evidence of shearing. They appear as light-coloured bands with respect to the parent rock and their thickness varies

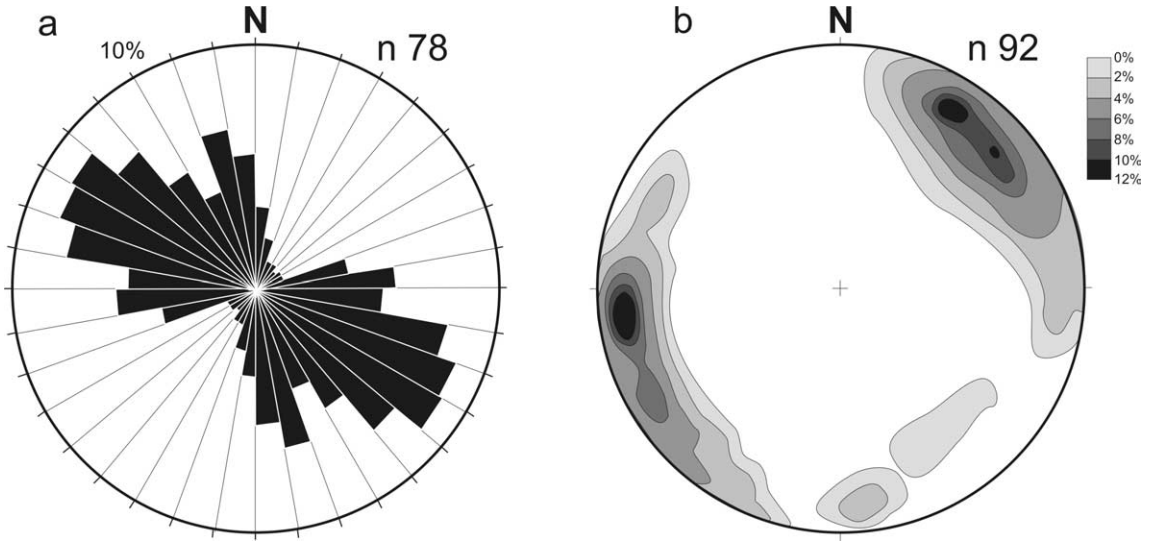

Fig. 5. (a) Rose diagram of the deformation bands' strike measured on the pavement. (b) Contoured stereonet plots (Schmidt net; lower hemisphere projection) of poles to sheared stylolites.

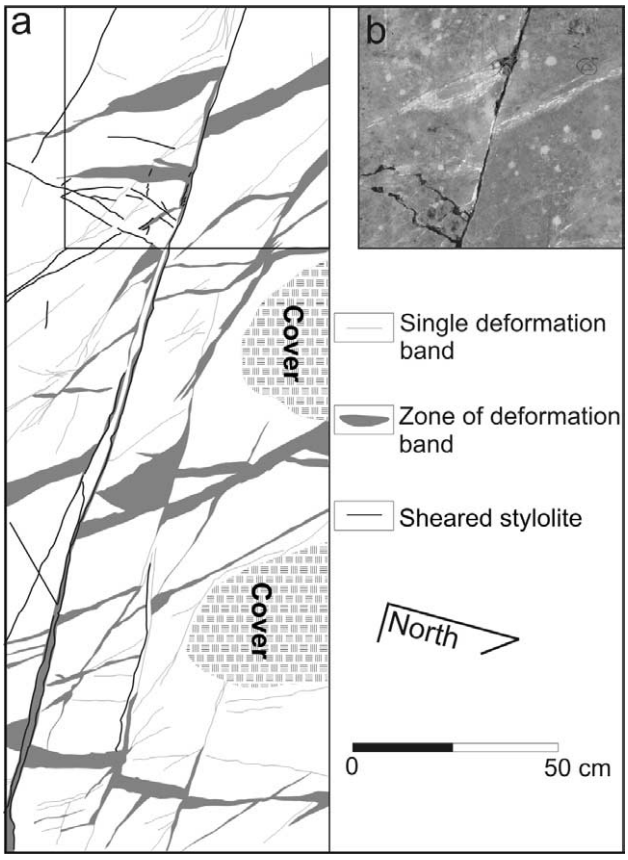

Fig. 6. (a) Line drawing of a network of deformation bands in three strike directions: N–NW, W–NW and E–W, and the overprinted stylolites. The E–W set cross-cuts and displaces all the other sets. (b) Photograph of the upper right part of the map (marked by rectangle in (a)), showing the east-striking sheared stylolite with 20 cm right lateral slip. Note that the sheared stylolite has a strong negative relief.

from 1 to 5 mm. The bed-parallel deformation bands are not developed extensively, and are made up of short, discontinuous segments.

Four of the younger sets of deformation bands show normal dip-slip components of motion and have mutually cross-cutting relationships, suggesting that they developed contemporaneously (Figs. 2 and 4).

These four groups form two pairs of conjugate sets; one striking N–NW and the other W–NW (Fig. 5). Among the N–NW striking sets, the E-dipping bands show a steeper dip angle (70–80°), whereas the W-dipping bands have a lower dip angle (50–60°) (Fig. 3). The W–NW-striking sets dip to the NE and to the SW at similar angles (60–70°). Another set of deformation bands trends E–W with an almost vertical dip angle and shows right-lateral strike-slip kinematics (Figs. 2, 5a and 6a). This set is the youngest, since it consistently displaces all the other structures described above.

All five of these sets of deformation bands include either single bands or zones of several individual bands (Figs. 3, 4 and 6a). These features are reminiscent of those of deformation bands in sandstone documented by Aydin and Johnson (1978). Single deformation bands are characterized by a thickness value between 1 and 2 mm and an offset between 1 and 2 mm. The zones of deformation bands with a normal sense of slip have a typical anastomosing pattern with interlinked eye and ramp structures (Fig. 4), as has been described in sandstone (see Antonellini and Aydin, 1995), whereas the zones of strike-slip deformation bands are straight and narrow (Figs. 6a and 7) and occasionally display a Riedel-like pattern (Ahlgren, 2001; Katz et al., 2004). Simple zones of deformation bands have thicknesses ranging from 2 mm to 5 cm and slip ranging from 2 mm to 5 cm.

Stylolites are generally associated with all six sets of deformation bands. One set of stylolites occurs parallel to the bedding, in many cases following the interface between the fine- and coarse-grained depositional fabric (Fig. 3b and c). Other sets consistently follow the deformation bands at an angle to bedding (Figs. 2 and 5b). In outcrop, stylolites commonly show a negative relief, due to erosion along the weaker residue material marking the structure (Fig. 6b). Detailed geometry of the stylolites, when visible, varies from columnar to wavy types. The band-parallel stylolites are commonly sheared, as evidenced by striated surfaces across which bedding and older structures are offset (Figs. 2 and 6b). The deformation bands and overprinted stylolites, with a cumulative offset of more than about 20 cm, form tabular zones of breccia and fine grained cataclastic fault rocks (gouge) which includes several slip surfaces (Figs. 8 and 9). These are the zones with the largest measured slip values (up to 75 cm). Considering that simple zones of deformation bands have limited offset (up to 5 cm), the presence of the zones of the assemblage (including deformation bands with overprinted sheared stylolites, cataclastic fault rock and slip surfaces) mark an advanced stage of fault development in the carbonate grainstone. Slip vs. thickness measurements of single bands and zones of deformation bands and complex fault zone assemblages are plotted in Fig. 10. The trends indicate that thickness–displacement relationships for both groups are more or less linear but a higher slope is evident for the assemblage.

Stylolites that are not associated with deformation bands occur only in central and northeastern parts of the quarry pavement (see Fig. 2). These stylolites strike N–NW and N–NE and are localized in the compressional quadrants of the main E–W striking right-lateral strike-slip zone of the assemblage. Some of these isolated stylolites show an interesting geometry when they cross pre-existing deformation bands (Fig. 11). They are deflected by the bands, that is, the stylolites became sub-parallel to the band for a short distance before diverging and resuming their original oblique orientation.

4. Thin section observations

Thin sections of the representative structural elements described above were examined using an optical microscope and secondary electron microscope (SEM). We sampled single deformation bands, zones of deformation bands and zones of deformation bands overprinted by sheared stylolites. It was difficult to sample intact stylolites and slip surfaces, because core samples tended to break apart along the stylolites and slip surfaces.

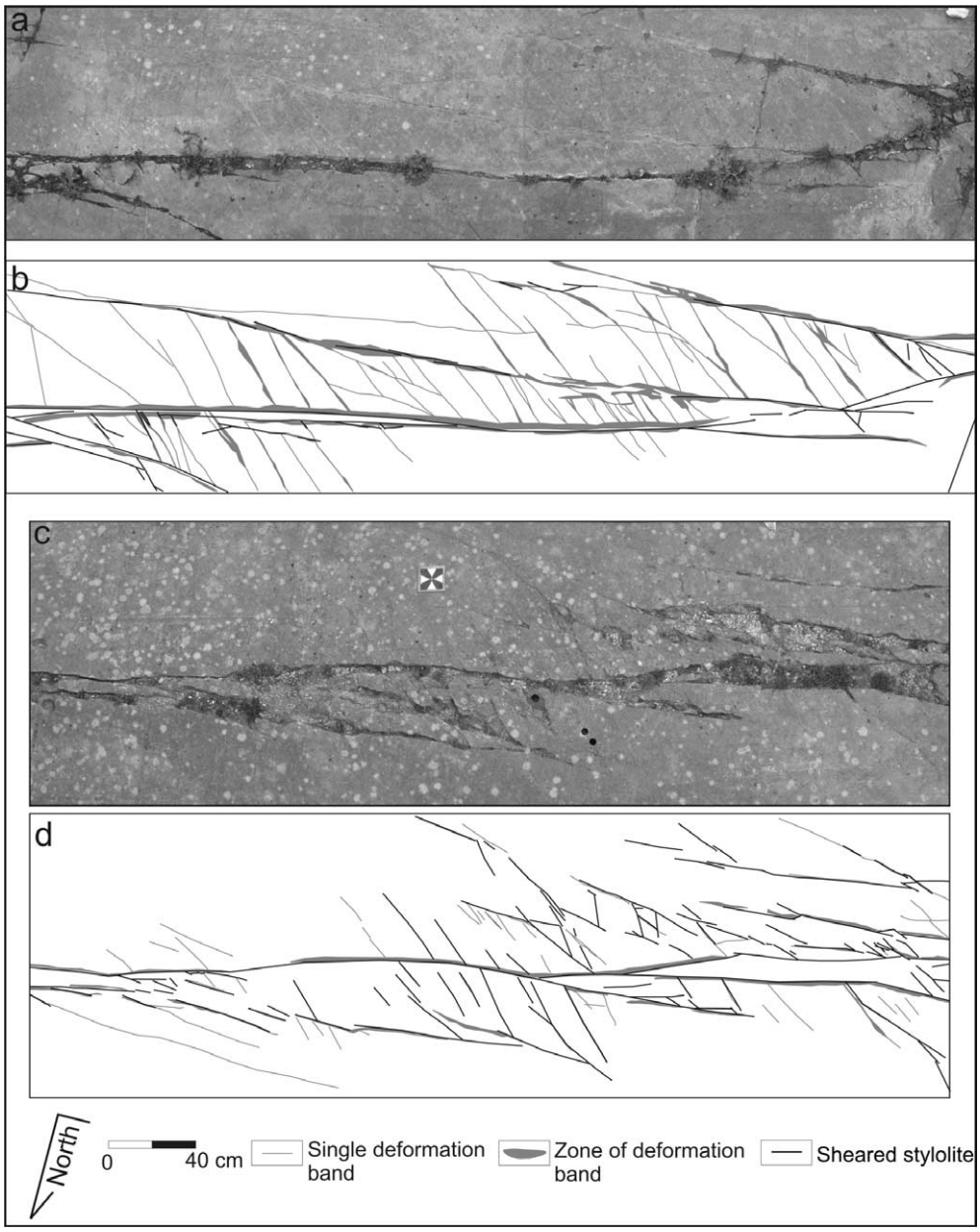

Fig. 7. Straight and narrow zones of strike-slip deformation bands. They display a razor blade-like or a Riedel-like pattern; (a) and (c) photographs, (b) and (d) maps.

4.1. Microstructural and textural characterization of deformation bands

We examined several samples of deformation bands and the associated structures, measuring porosity and grains-to-matrix percentage within the bands, in both the boundary region of the bands and in the surrounding host rock (samples numbered 1–20 in the first row of Table 1). After the construction of accurate maps from thin sections photographs, the measured values have been determined using an automatic pixel counting with a resolution less than 1%.

The host rock is a poor-to-medium consolidated grainstone. Grains are made up of fragments of rudist and range in size from 0.05 to 0.4 mm (Fig. 12a and b) and make up about 53% of the rock volume. The matrix consists of bladed and sparry calcite cement, microspherules of silica cement and rudist fragments smaller than 0.05 mm (see also Mutti, 1995) and makes up about 25% of the rock (Table 1). The average porosity is about 22%. The values of the grains-to-matrix ratio in the host rock fall between 1.7 and 2.5, with porosities from 15 to 28%. The thin section images of single deformation bands, occurring parallel and oblique to the bedding, show strikingly different texture and petrophysical properties with respect to the parent rock. The inner parts of single deformation bands (Fig. 12c–e) are characterized by low porosity on the order of 1–4% (Table 1). However, they maintain the same ratio of grains to matrix, indicating no grain size reduction occurred (see the bottom row of Table 1).

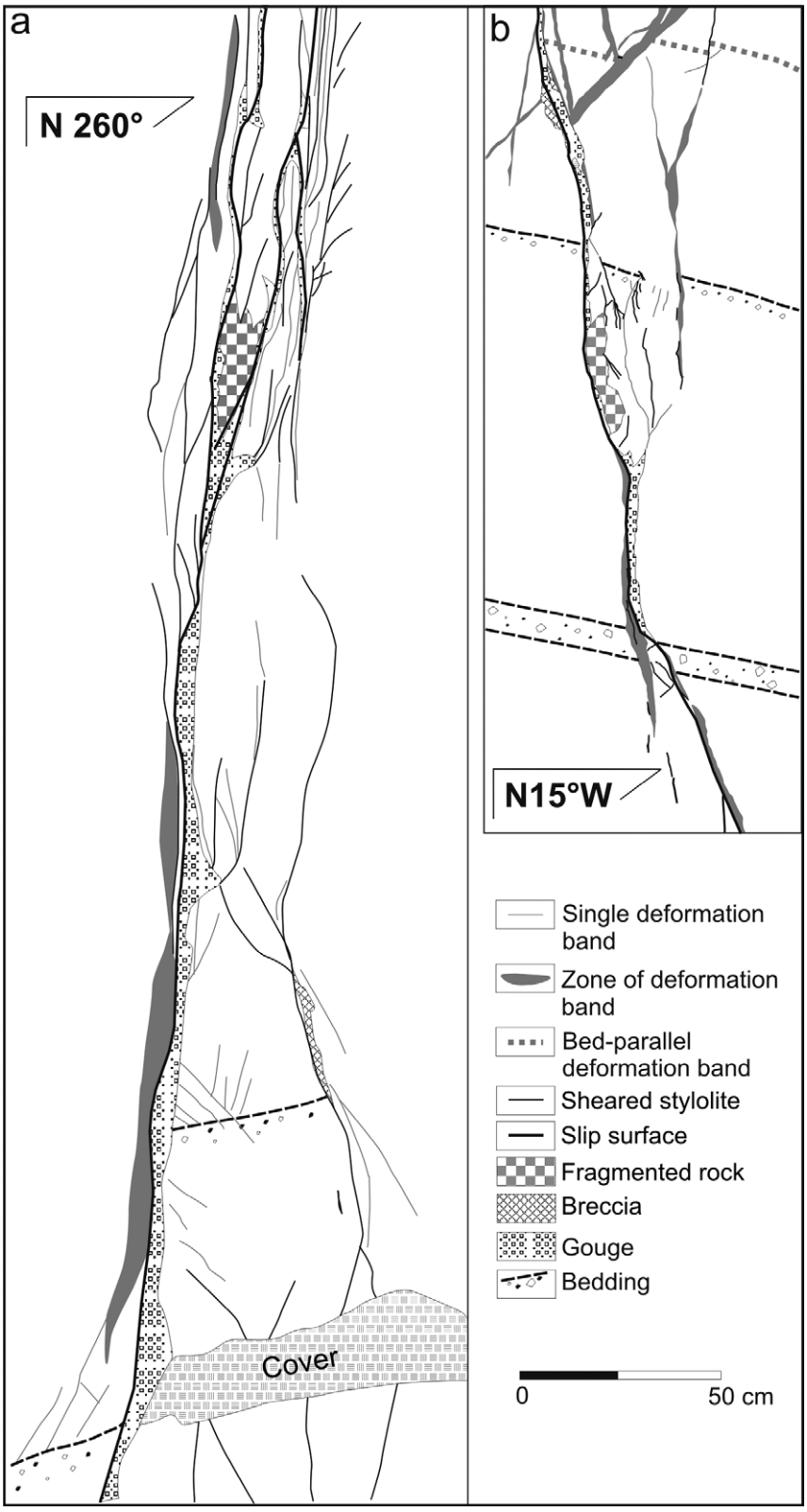

Fig. 8. Line drawings of the main N–NW-striking dip-slip deformation bands on the southern wall (a) and of the main E–W-striking right-lateral fault zone, on the western wall (b). The zone includes the entire assemblage; deformation bands, sheared stylolites, fault rock (breccia and gouge) and slip surfaces.

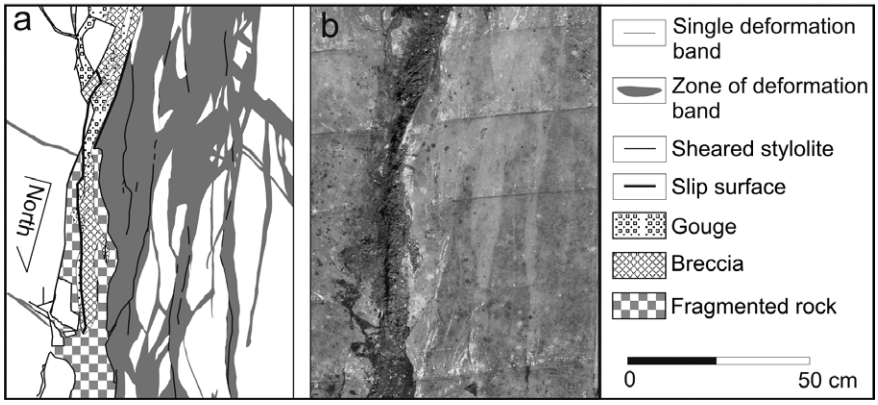

Fig. 9. Line drawings (a) and photograph (b) of the main N–NW-striking dip-slip fault characterized by a complex assemblage composed of slip surfaces, a zone of deformation bands and two sets of stylolites, the band-parallel sheared stylolites and the oblique stylolites set.

The inner parts of the deformation bands are bounded on both sides by an area usually measuring one-half the band thickness (termed the 'boundary zone' in Antonellini and Aydin (1994)), where pore volume change is less than that in the inner band itself. The boundary zone is characterized by a moderate porosity ranging from 7 to 14% (see Table 1).

Deformation bands (Fig. 13a) are in most cases overprinted by stylolites. All stylolites are marked by a ~0.001–0.01-mm-thick dark material showing columnar and wavy form with average amplitude of 0.01 mm. This dark material was analyzed for elemental composition using SEM and it was found to be characterized by high proportions of organic carbon (C), with low amounts of calcium (Ca) and oxygen (O) (Fig. 13b).

We were able to observe, in a deformation band oriented oblique to the bedding, a set of stylolites oriented nearly parallel to the band boundaries, which represent the simplest association of deformation band-stylolites in thin section study. These stylolites are accompanied by a few thin and discontinuous pockets of reduced grain size, perhaps representing the incipient process of cataclasis (Fig. 14a and b). The band-parallel stylolites appear to be sheared, based on the presence of a second set of short and poorly developed oblique stylolites. In another case, a well-developed, continuous zone of grain size and porosity reduction is identifiable (Fig. 14c and d). In terms of petrophysical properties, this zone is similar to the cataclastic deformation zones described in earlier studies (Engelder, 1974; Aydin, 1978).

In thicker zones of deformation bands representing more complex cases, more than two sets of stylolites are detected. For example, the images in Fig. 14e and f show at least two more sets of stylolites oriented obliquely to the bands, in addition to the band-parallel set of stylolites. The presence of multiple sets of stylolites indicates a complex history of slip across the thicker zones, resulting in the comminution of carbonate rock. In particular, the band-parallel set of stylolites must have been sheared to produce the shorter oblique stylolites. As shown by an isolated rudist fragment that survived within a cataclastic zone (Fig. 15), the main process by which the size reduction of the rudist fragments occurs is pressure solution leading to multiple sets of intersecting stylolites. The cataclastic material produced by this process has the lowest grains-to-matrix ratio (0.2–0.5) with respect to bands without cataclasis (1.4–2.5), as well as the lowest porosity (less than 1%; Table 1). These grain size and porosity reductions represent an advanced stage of deformation and

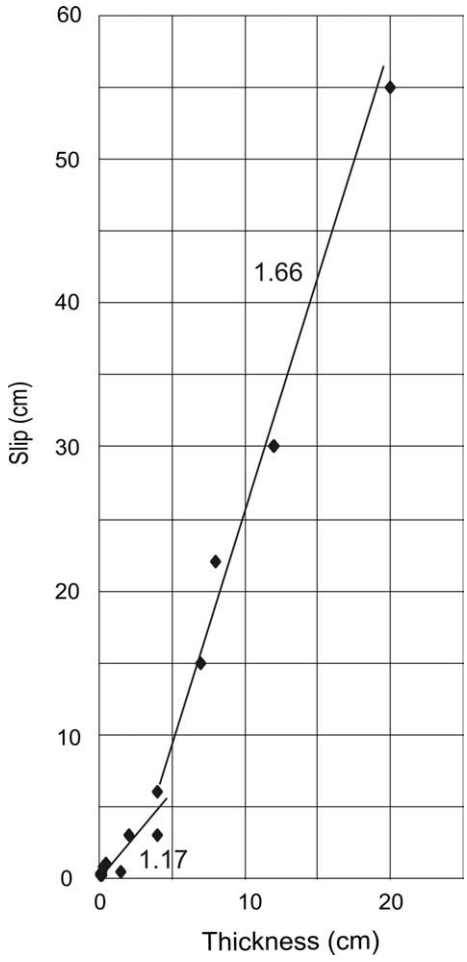

Fig. 10. Slip vs. thickness relationship of single deformation bands, zone of deformation bands with the associated sheared stylolites and slip surfaces defining two populations.

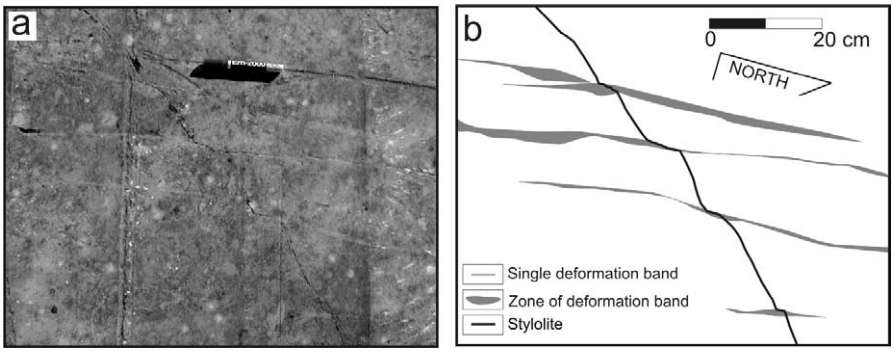

Fig. 11. Photograph (a) and map (b) of a stylolite plane being deflected by several subparallel zones of deformation bands where the stylolite tends to cut across them.

sometimes occur in a few adjacent sub-parallel cataclastic zones (Fig. 14e and f). In Fig. 14c and e, immediately adjacent to these sub-parallel cataclastic zones containing multiple sets of intersecting stylolites, a few coarse grains appear to have twinning in the calcite minerals similar to that reported by Ferrill and Groshong (1993), in low-porosity limestones.

Data on the relative percentage of pores, grains and matrix collected from samples representing progressive deformation stages are plotted on a triangular diagram in Fig. 16. These data show an evolving deformation path, from the boundary zone of deformation bands to deformation bands without cataclasis and finally to the deformation bands with cataclasis.

5. Discussion

In the Madonna della Mazza quarry, the oldest structures are bed-parallel deformation bands. These bands lack any evidence of shearing and are similar to other deformation bands. Therefore, we interpret these structures as compaction bands. We also suggest that the bed-parallel compaction bands formed during burial at overburden pressures ranging from 10 to 70 MPa corresponding to about 0.5–3.0 km of overburden (Ori et al., 1986; Mutti, 1995). The high porosity coarse-grained beds (up to 30% and possibly 47% skeleton porosity) of the grainstones are the preferred locations for the compaction bands (Fig. 3c). These estimates of porosity and range of overburden pressure are consistent with experimental results obtained from limestones showing comparable properties, pore collapse and compaction localization (fig. 5a in Vajdova et al., 2004). The timing of compaction with respect to the calcite cementation, however, is not well established. If the bands formed prior to cementation, the skeleton porosity (~47%) should be the relevant parameter, then we conclude that lithostatic pressures are lower than those referred to above for the critical pore collapse mechanism.

Compaction bands oriented at an angle to the bedding in sandstone have been described in previous studies (Hill, 1989; Mollema and Antonellini, 1996) and they have been defined as end members of volumetric deformation bands (Aydin et al., in press). However, this is the first time that a set of compaction bands parallel to bedding in any type of layered rock has been reported.

The other five sets of deformation bands, oriented at various angles to the bedding, show both porosity reduction and shearing and are, therefore, classified as compactive shear bands, according to framework proposed by Bésuelle (2001); Aydin et al. (in press). Among these, single compactive shear bands with no stylolites or cataclasis represent the simplest fundamental shear structure formed in the porous carbonate grainstone (Fig. 17a). The mechanism of compactive shear bands appears to be particulate flow involving grain translation and rotation with pore collapse, resulting in a tight band with a noticeable shear displacement gradient but without significant grain breakage. This mechanism has been observed in several limestones with a wide range of porosity (3–45%) deformed in the laboratory under low-to-high mean stresses, ranging from 11 to 450 MPA (Baud et al., 2000; Vajdova et al., 2004). The laboratory results also show that the higher end of porosities required lower critical confining pressures for the compactive process to occur by pore collapse. These results are consistent with the estimated initial high porosity (15–30%) and/or skeleton porosity (~47%) of the Orfento Formation and

Table 1
Grains, matrix and porosity percentage in the host rock, in the boundary region of deformation bands and within the deformation bands (with and without cataclasis). The ratio between grain and matrix is also shown. Mean error is on the order of 1%

	Host rock					Boundary					Bands									
											Without cataclasis					With cataclasis				
Sample no.	1	2	3	4	5	6	7	8	9	10	11	12	13	14	15	16	17	18	19	20
Grains (%)	54.8	51.0	60.3	47.0	52.5	63.5	57.4	54.5	56.6	58.0	64.1	56.2	71.2	57.7	59.0	21.4	34.3	17.7	26.8	30.3
Matrix (%)	23.3	30.3	24.4	24.5	22.5	22.9	29.0	37.0	36.3	30.4	31.8	42.0	28.0	41.3	39.0	78.0	65.0	81.9	72.4	69.6
Porosity (%)	21.9	18.7	15.3	28.5	25.0	13.6	13.6	8.5	7.1	11.6	4.1	1.8	0.8	0.9	2.0	0.6	0.7	0.4	0.8	0.1
Grain/ matrix	2.3	1.7	2.5	1.9	2.3	2.8	2.0	1.5	1.6	1.9	2.0	1.4	2.5	1.4	1.5	0.3	0.5	0.2	0.4	0.4

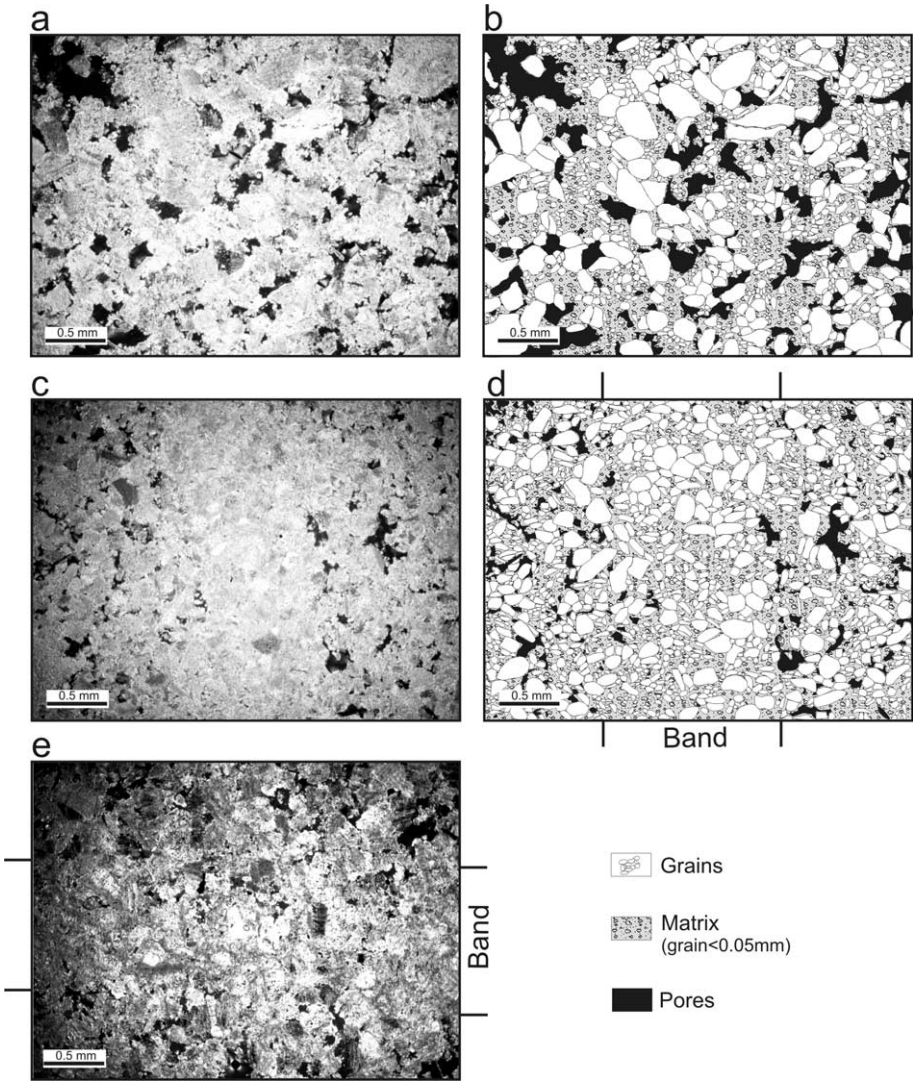

Fig. 12. The host rock is composed of fragments of rudist and matrix. Porosity ranges between 15 and 30%; (a) photograph and (b) map. Single deformation bands with no cataclasis, occurring oblique, (c) photograph and (d) map, and parallel (e) to the bedding. In the inner parts of the bands, porosity ranges between 1 and 4%.

relatively low overburden thickness during its burial history (Mutti, 1995).

Stylolites are generally characterized by typical columnar forms and are compositionally high in organic carbon and low in calcium and oxygen. The organic material is due to either residue from the dissolution of rudist shale or to the flow of hydrocarbons through the parting of solution seams as it occurs in several localities in Majella Mountain. The bed-parallel stylolites occur adjacent to bed-parallel compaction bands and follow the interface between the coarse- and fine-grained fabric. Even though these structures are produced by different processes, they are kinematically compatible. Therefore, the transition from one mode to another does not require drastic changes in loading conditions.

Band-parallel stylolites located inside the earlier compactive shear bands, however, pose a slightly different problem, in the sense that the former represent a principal stress plane, whereas the latter were presumed to be formed in an orientation subjected to some combination of shear and compressive normal stresses (Aydin et al., in press). In addition, the pressure solution process responsible for the stylolites takes place within the shear band material that has already been significantly compacted (Fig. 17b). This suggests that the transition from compactive shear band localization to stylolitic pressure solution involves rheological, as well as loading, changes.

First we consider the impact of the changing material properties on the transition from particulate flow and pore collapse to pressure solution. The porosity in the band has been reduced from 15% minimum measured porosity and 47% calculated skeleton porosity to 1–4%. This reduction in porosity, together with the interlocking of the grains, may shift the mechanical behaviour from one that was controlled by weak Hertzian contact forces to a solid-like behaviour with a high M-modulus (ρV_p^2) (Dvorkin and Nur, 1996), thereby enhancing the processes of pressure solution and formation of through-going stylolites.

The occurrence of band-parallel stylolites along all five sets of compactive shear bands is curious and cannot be explained

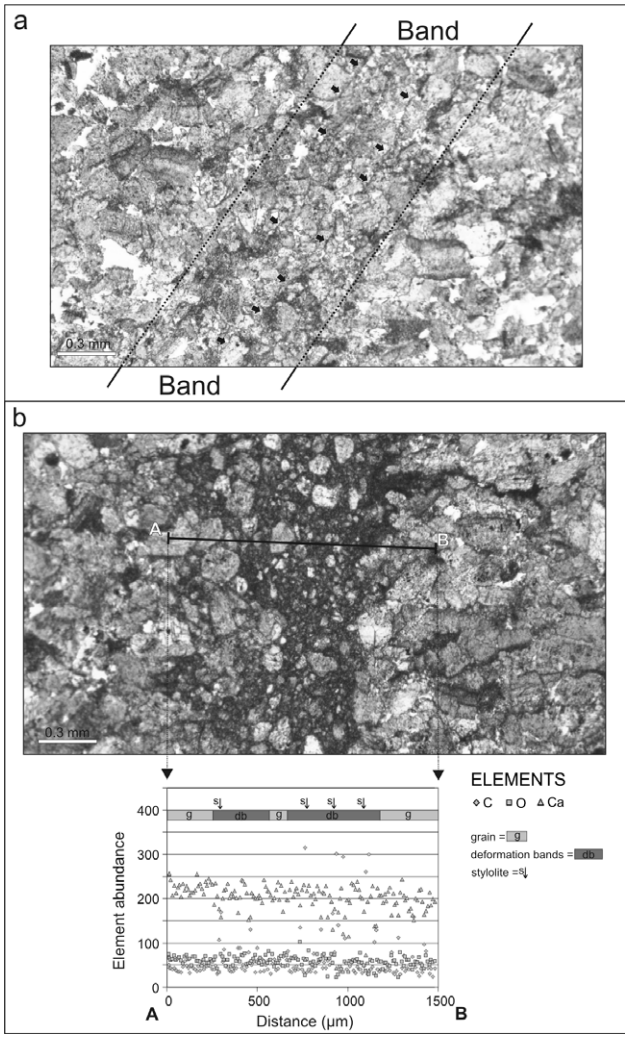

Fig. 13. Single deformation band with stylolites (marked by arrows) (a). Elemental compositions and relative abundance across a deformation band overprinted by stylolites as determined using SEM (b). The dark material within stylolites is characterized by high amounts of organic carbon (C) and low amounts of calcium (Ca) and oxygen (O). On photographs, pores are white.

solely by rheological changes. Considering that stylolites are analogues of anti-cracks (Fletcher and Pollard, 1981) and form perpendicular to the greatest compression, the observed geometric relationships may indicate that the remote stress system responsible for compactive shear banding has changed several times, such that the greatest compressive stresses have become perpendicular to each set of bands at certain times. However, it is difficult to imagine that such changes would take place with such a high frequency. Furthermore, each set of stylolites was later sheared, requiring additional changes in the loading system. Alternatively, the local stresses may have changed due to the rheological anisotropy introduced by material with a high M-modulus within the compactive shear bands. This possibility is evident in the deflection of a stylolite from an oblique orientation to a band-parallel orientation while it crosses four compactive shear bands (Fig. 11). This notion is similar to the strain partitioning mechanism described by several workers including Borradaile and Tarling (1984), Groshong et al. (1984) and Gross (1995).

In any case, shearing of the stylolites required additional changes such that the stylolites, originally in anti-crack mode along a principal plane orientation, became subjected to shearing. It is interesting to note that the senses of shearing on the sheared stylolites are the same as those associated with the compactive shear bands. Also, slip along the band-parallel stylolites resulted in formation of an oblique set of stylolites, concentrated at the contractional quadrant of the sheared stylolites (Fig. 17c) (Rispoli, 1981; Graham et al., 2003). Increased slip along the band-parallel, sheared stylolites, together with shearing of the increased number of oblique sets of stylolites, fragmented the rock and produced a fine-grained zone of cataclasis (Fig. 17c and d). It has been previously noted that cataclasis in compactive deformation bands in sandstone is a consequence of opening mode fractures and grain crushing (Engelder, 1974; Aydin, 1978; Wong et al., 1990), whereas here, grain size reduction occurs solely by a pressure solution process and the resulting discrete stylolites (anti-cracks) and their subsequent shearing.

The compaction bands and stylolites that are oriented parallel to the bedding represent pretilting structures. The four sets of compactive shear bands with normal components of motion form two pairs of conjugate sets that could also be pretilting (Van Dijk et al., submitted for publication), based on the high porosity–low confining pressure inferred from the particulate flow mechanism of the deformation, or they could, alternatively, be associated with tilting of strata and the flexural slip. This later mechanism is similar to that proposed by Graham et al. (2003) for the southern part of the Majella anticline. There, the youngest set of right-lateral strike-slip faults is presently vertical and cuts across inclined beds, suggesting that they represent post-tilting deformations (Cello et al., 1997; Di Bucci and Mazzoli, 2002; Tondi et al., in press).

The structures described here are also important for fluid flow. It is well known that compaction bands and compactive shear bands in sandstone have lower porosity and permeability (Antonellini and Aydin, 1994; Sternlof et al., 2004). Similarly, Van Dijk et al. (submitted for publication), focusing on the fluid flow properties of the fault in the Madonna della Mazza quarry, determined that they have low permeability with respect to the host rock and may compartmentalize a reservoir or aquifer in the subsurface.

6. Conclusions

In this study, we document, through detailed mapping and microstructural and textural analyses, fault development in porous carbonate grainstone of the Orfento Formation exposed in a quarry in the northwest part of the Majella Mountains in central Italy.

We have identified three major processes that played an important role in this development:

1. strain localization into narrow bands;
2. pressure solution; and
3. shearing of pressure solution products, that is, shearing of stylolites.

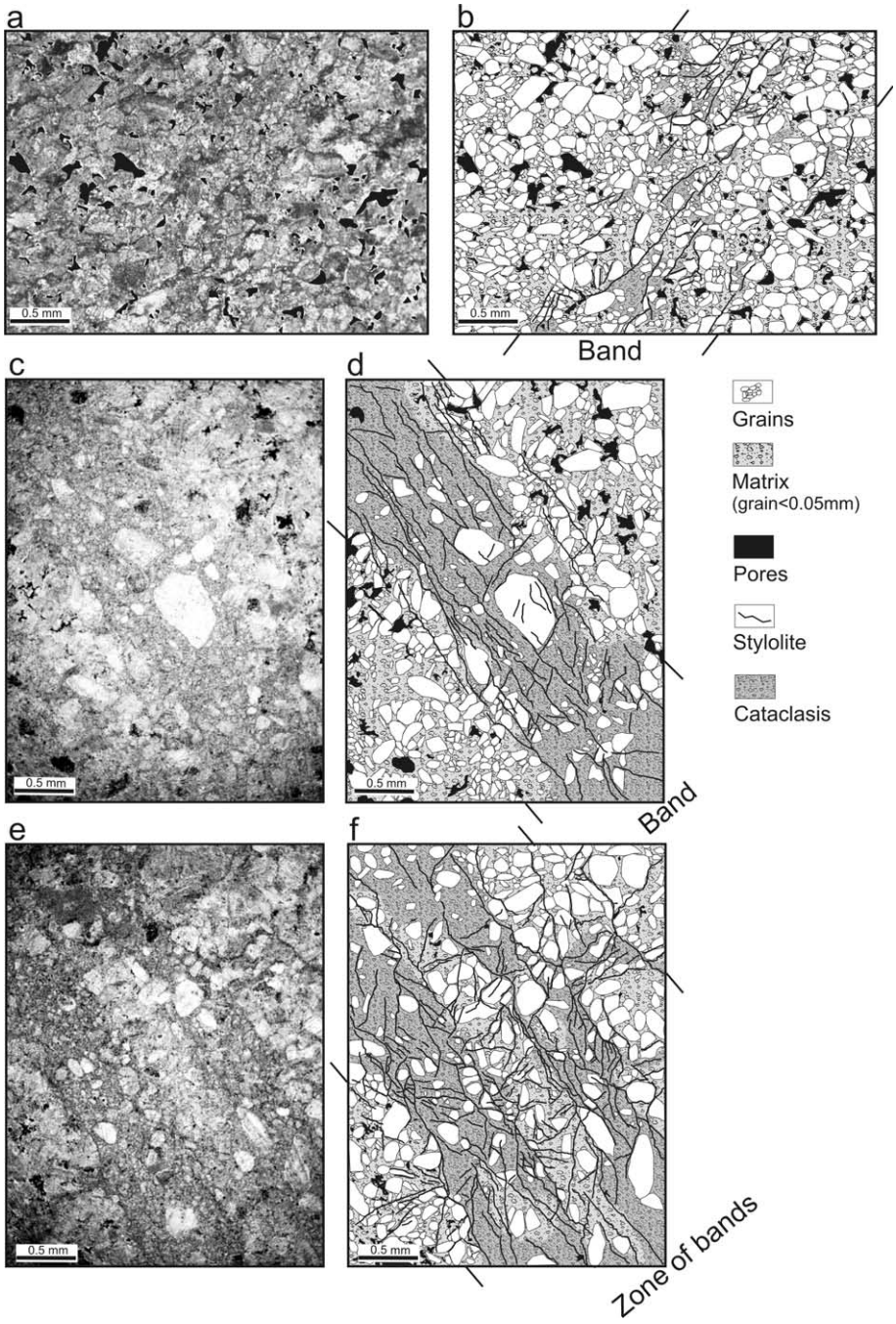

Fig. 14. Single deformation band with stylolites and discontinuous pockets of cataclasis; (a) photograph and (b) map. Single deformation bands, (c) photograph and (d) map, characterized by continuous tabular zone of cataclasis. Small zone of deformation bands, (e) photographs and (f) map, characterized by tabular zones of cataclasis separated by less deformed rock. Different sets of oblique stylolites are present within the bands and less deformed lenses of parent rock.

The products of the first process are bed-parallel compaction bands and five sets of compactive shear bands that are characterized by a particulate flow mechanism involving grain rotation, translation and pore collapse. The occurrence of bed-parallel compaction bands, in general, and their formation in carbonates, in particular, is reported for the first time in this paper.

The products of the pressure solution process are one set of bed-parallel stylolites and five major sets of stylolites, each overprinting the earlier individual sets of compactive shear bands. The shearing of these stylolites produce secondary and tertiary sets of stylolites oblique to the compactive shear bands and the sheared stylolites, all of which help to reduce the grain size and form a cataclastic narrow zone within the band. A plot of slip vs. thickness for the faults exposed in the quarry shows that larger slip values correspond to those faults with sheared stylolites and the resulting cataclastic fault rock. These progressions indicate an evolving fault growth process in carbonates. Overprinting failure mechanisms from deformation banding to opening mode fracturing and subsequent shearing have been previously recognized in sandstone (Zhao

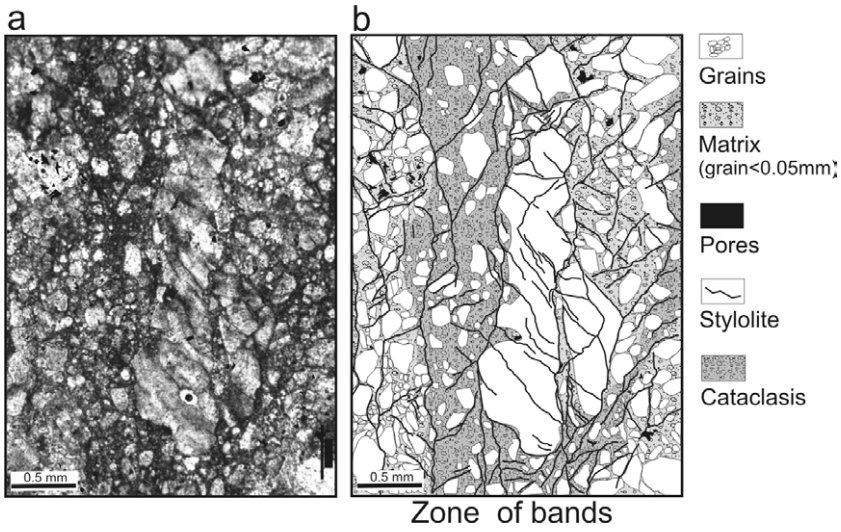

Fig. 15. Isolated rudist fragment within a cataclastic zone. The occurrence of oblique sets of stylolites is the main process responsible for reduction in grain size; (a) photograph and (b) map.

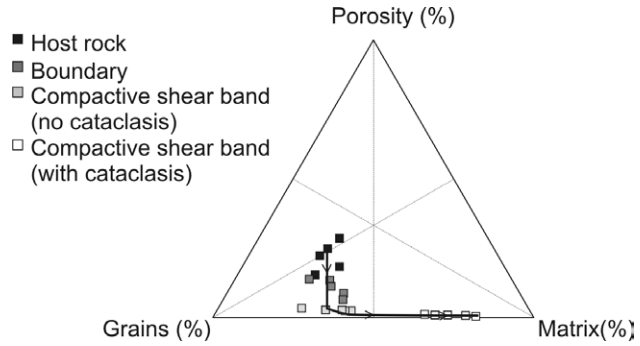

Fig. 16. Percentage of pores, grains and matrix of deformation bands. Line with arrows depicts the deformation path.

and Johnson, 1992; Davatzes and Aydin, 2003). This is the first time that a series of interactive failure processes involving strain localization into bands, pressure solution and subsequent shearing and cataclasis has been reported in carbonates.

The transitions from one deformation process to another pose intriguing questions and are likely controlled by changing of material properties within the bands, the anisotropy resulting from these changes and possible changes in the orientation and magnitude of applied stresses. These problems, and their structural framework with respect to the Majella thrust sheet, remain to be subjects for further studies.

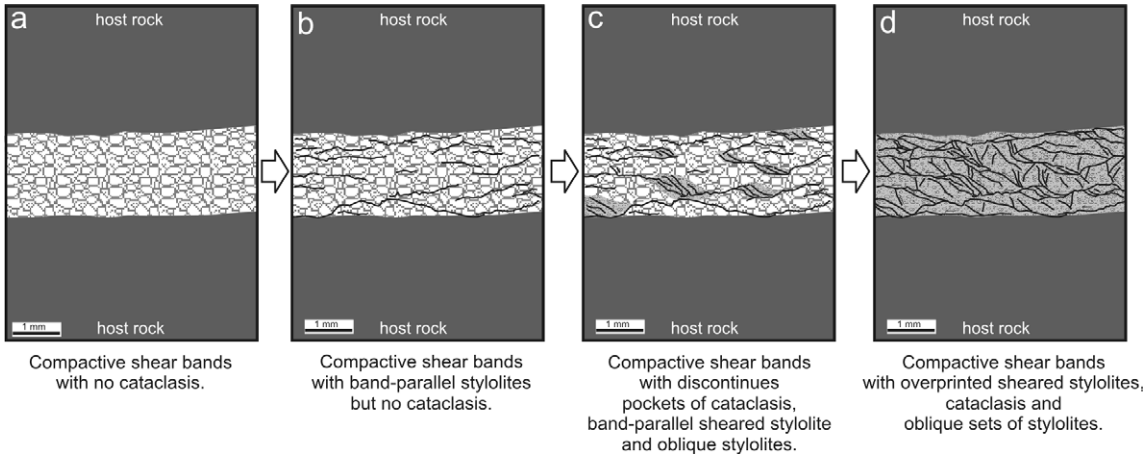

Fig. 17. Evolution of faults within the compactive shear bands in the carbonate grainstone of the Orfento Formation. Black lines represent the different sets of stylolites and/or sheared stylolites. In (c), discontinuous pockets of cataclasis are highlighted in grey.

Acknowledgements

This work has been supported by University of Camerino (research funds to E. Tondi), by the MIUR, Cofin 2002 (research funds to G. Cello), and by the Rock Fracture Project at Stanford University (research funds for A. Aydin and M. Antonellini). We thank Fabrizio Agosta for useful discussions during field work and during the preparation of the manuscript and Ramil Ahmadov for his help in the laboratory and with image analysis.

References

Ahlgren, S.G., 2001. The nucleation and evolution of Riedel shear-zones as deformation bands in porous sandstone. Journal of Structural Geology 23, 1203–1214.

Alvarez, W., Engelder, T., Geiser, P.A., 1978. Classification of solution cleavage in pelagic limestones. Geology 6, 263–266.

Antonellini, M.A., Aydin, A., 1994. Effect of faulting on fluid flow in porous sandstones: petrophysical properties. American Association of Petroleum Geologists Bulletin 78, 355–377.

Antonellini, M.A., Aydin, A., 1995. Effect of faulting on fluid flow in porous sandstones: geometry and spatial distribution. American Association of Petroleum Geologists Bulletin 79, 642–671.

Antonellini, M.A., Aydin, A., Pollard, D.D., 1994. Microstructure of deformation bands in porous sandstones at Arches National Park, Utah. Journal of Structural Geology 16, 941–959.

Aydin, A., 1978. Small faults formed as deformation bands in sandstone. Pure and Applied Geophysics 116, 913–930.

Aydin, A., Johnson, A.M., 1978. Development of faults as zones of deformation bands and as slip surfaces in sandstone. Pure and Applied Geophysics 116, 931–942.

Aydin, A., Borja, R.I., Eichhubl, P., in press. Geological and mathematical framework for failure modes in granular rock. Journal of Structural Geology.

Baud, P., Schubnel, A., Wong, T.F., 2000. Dilatancy, compaction, and failure mode in Solnhofen limestone. Journal of Geophysical Research—Solid Earth 105 (B8), 19289–19303.

Bésuelle, P., 2001. Compacting and dilating shear bands in porous rock: theoretical and experimental conditions. Journal of Geophysical Research 106, 13,435–13,442.

Billi, A., Salvini, F., Storti, F., 2003. The damage zone-fault core transition in carbonate rocks: implications for fault growth, structure and permeability. Journal of Structural Geology 25, 1779–1794.

Borradaile, G.J., Tarling, D., 1984. Strain partitioning and magnetic fabrics in particulate flow. Canadian Journal of Earth Sciences 21 (6), 694–697.

Cello, G., Mazzoli, S., Tondi, E., Turco, E., 1997. Active tectonics in the Central Apennines and possible implications for seismic hazard analysis in peninsular Italy. Tectonophysics 272, 43–68.

Davatzes, N.C., Aydin, A., 2003. Overprinting faulting mechanisms in sandstone. Journal of Structural Geology 25, 1795–1813.

Di Bucci, D., Mazzoli, S., 2002. Active tectonics of the Northern Apennines and Adria geodynamics: new data and a discussion. Journal of Geodynamics 34 (5), 687–707.

Dvorkin, J., Nur, A., 1996. Elasticity of high-porosity sandstones: theory for two North Sea data sets. Geophysics 61, 1363–1370.

Eberli, G.P., Bernoulli, D., Sanders, D., Vecsei, A., 1993. From aggradation to progradation: the Majella platform (Abruzzi, Italy). In: Simo, T., Scott, R.W., Masse, J.P. (Eds.), Atlas of Cretaceous Carbonate Platforms American Association of Petroleum Geologists Memoir 56, pp. 213–232.

Engelder, T., 1974. Cataclasis and the generation of fault gouge. Geological Society of America Bulletin 85, 1515–1522.

Engelder, T., Marshak, S., 1985. Disjunctive cleavage formed at shallow depth in sedimentary rocks. In: Hancock, P.L., Powell, C.M. (Eds.), Multiple Deformation in Ductile and Brittle Rocks. Pergamon, New York, pp. 327–343.

Ferrill, D.A., Groshong Jr., R.H., 1993. Deformation conditions in the northern Subalpine Chain, France, estimated from deformation modes in coarse-grained limestone. Journal of Structural Geology 15, 995–1006.

Fletcher, R.C., Pollard, D.D., 1981. Anticrack model for pressure solution surfaces. Geology 9, 419–424.

Ghisetti, F., Vezzani, L., 2002. Normal faulting, extension and uplift in the outer thrust belt of the central Apennines (Italy): role of the Caramanico fault. Basin Research 14, 225–236.

Graham, B., Antonellini, M., Aydin, A., 2003. Formation and growth of normal faults in carbonates within a compressive environment. Geology 31, 11–14.

Groshong, R.H., 1988. Low-temperature deformation mechanisms and their interpretation. Geological Society of America Bulletin 100, 1329–1360.

Groshong, R.H., Pfiffner, O.A., Pringle, L.R., 1984. Strain partitioning in the Helvetic thrust belt of eastern Switzerland from the leading-edge to the internal zone. Journal of Structural Geology 6 (1-2), 5–18.

Gross, M.R., 1995. Fracture partitioning - failure mode as a function of lithology in the Monterey Formation of coastal California. Geological Society of America Bulletin 107 (7), 779–792.

Hill, R.E., 1989. Analysis of deformation bands in the Aztec Sandstone, Valley of Fire, Nevada. M.S. thesis, Geosciences Department, University of Nevada, Las Vegas.

Jamison, W.R., Stearns, D.W., 1982. Tectonic deformation of Wingate Sandstone, Colorado National Monument. AAPG Bulletin 66, 2584–2608.

Katz, Y., Weinberger, R., Aydin, A., 2004. Geometry and kinematic evolution of Riedel shear structures, Capitol Reef National Park, Utah. Journal of Structural Geology 26 (3), 491–501.

Lampert, S.A., Lowrie, W., Hirt, A.M., Bernoulli, D., Mutti, M., 1997. Magnetic and sequence stratigraphy of redeposited Upper Cretaceous limestones in the Montagna della Maiella, Abruzzi, Italy. Earth and Planetary Science Letters 150, 79–83.

Mair, K., Main, I., Elphick, S., 2000. Sequential growth of deformation bands in the laboratory. Journal of Structural Geology 22, 25–42.

Marchegiani, L., Van Dijk, J.P., Gillespie, P.A., Tondi, E., Cello, G., in press. Scaling properties of the dimensional and spatial characteristics of fault and fracture systems in the Majella Mountain, central Italy. Geological Society, London, Special Publications.

Mollema, P.N., Antonellini, M.A., 1996. Compaction bands: a structural analog for anti mode I cracks in aeolian sandstone. Tectonophysics 267, 209–228.

Mutti, M., 1995. Porosity development and diagenesis in the Orfento supersequence and its bounding unconformities (Upper Cretaceous, Montagna Della Majella, Italy). American Association of Petroleum Geologists Special Publications, 141–158.

Ori, G.G., Roveri, M., Vannoni, F., 1986. Plio-Pleistocene sedimentation in the Apennine–Adriatic foredeep (central Adriatic Sea, Italy). In: Allen, P.A., Homewood, P. (Eds.), Foreland Basins. Blackwell, Oxford, pp. 183–198.

Peacock, D.C.P., Sanderson, D.J., 1995. Pull-aparts, shear fractures and pressure solution. Tectonophysics 241, 1–13.

Rispoli, R., 1981. Stress field about strike-slip faults inferred from stylolites and tension gashes. Tectonophysics 75, 29–36.

Rutter, E.H., 1983. Pressure solution in nature, theory and experiment. Geological Society of London Journal 140, 725–740.

Salvini, F., Billi, A., Wise, D.U., 1999. Strike-slip fault-propagation cleavage in carbonate rocks: the Mattinata Fault zone, Southern Apennines, Italy. Journal of Structural Geology 21, 1731–1749.

Scisciani, V., Tavarnelli, E., Calamita, F., 2002. The interaction of extensional and contractional deformation in the outer zones of the Central Apennines, Italy. Journal of Structural Geology 24, 1647–1658.

Shipton, Z.K., Cowie, P.A., 2001. Damage zone and slip-surface evolution over (m to km scales in high-porosity Navajo sandstone, Utah. Journal of Structural Geology 23, 1825–1844.

Sternlof, K.R., Chapin, J.R., Pollard, D.D., Durlofsky, L.J., 2004. Permeability effects of deformation band arrays in sandstone. AAPG Bulletin 88 (9), 1315–1329.

Tondi, E., Piccardi, L., Cacon, S., Kontny, B., Cello, G., 2005. Structural and time constraints for dextral shear along the seismogenic Mattinata Fault (Gargano, southern Italy). Journal of Geodynamics 40, 134–152.

Vajdova, V., Baud, P., Wong, T.F., 2004. Compaction, dilatancy, and failure in porous carbonate rocks. Journal of Geophysical Research—Solid Earth 109 (B5). Art. No. B05204.

Van Dijk, J.P., Gillespie, P., Rawnsley, K., Ameen, M., Cello, G., Petit, J.P., et al., 2002. A New Faulting Mechanism in Carbonate Rocks. Examples From Majella Mountain Anticline, Italy SFERA Inaugural Meeting 2002, Abstracts Volume, Paper 9, pp. 46–49.

Van Dijk, J.P., Cello, G., Gillespie, P., Marchegiani, L., submitted for publication. Fault populations and permeability analysis in porous carbonate grainstones; the Madonna della Mazza Quarry, Majella Mountain, Italy. Journal of Structural Geology.

Willemse, E.J.M., Peacock, D.C.P., Aydin, A., 1997. Nucleation and growth of strike-slip faults in limestones from Somerset, U.K.. Journal of Structural Geology 19, 1461–1477.

Wong, T.-F., 1990. Deformation Mechanisms, Rheology and Tectonics. Geological Society Special Publications, pp.111–122.

Zhao, G., Johnson, A.M., 1992. Sequence of deformation recorded in joints and faults, Arches National Park, Utah. Journal of Structural Geology 14, 225–236.